JOURNAL OF GEOPHYSICAL RESEARCH, VOL. 100, NO. B8, PAGES 15,717–15,734, AUGUST 10, 1995

Syntectonic generation and segregation of tonalitic melts from amphibolite dikes in the lower crust, Striding-Athabasca mylonite zone, northern Saskatchewan

M. L. Williams
Department of Geology and Geography, University of Massachusetts, Amherst

S. Hanmer
Continental Geoscience Division, Geological Survey of Canada, Ottawa, Ontario

C. Kopf and M. Darrach
Department of Geology and Geography, University of Massachusetts, Amherst

Abstract. Vapor-absent melting in a swarm of amphibolite dikes in the lower crust has produced segregations of tonalitic and trondhjemitic composition in a variety of textures and structures that dramatically illustrate the mechanisms of melt segregation during deformation. The 3.2 Ga Chipman dikes intrude the mylonitized Chipman tonalite within the Striding-Athabasca mylonite zone of northern Saskatchewan. Dike emplacement spans a major sinistral transpressive ductile deformation and granulite facies metamorphic event. Older dikes are intensely folded and sheared; younger dikes are undeformed. Major and trace element analyses indicate that the dikes are tholeiitic basalts, similar in composition to mid-ocean ridge basalt. Thermobarometry finds conditions of 750-850°C, 1.0 GPa. The youngest, most pristine dikes contain hornblende and plagioclase with minor clinopyroxene and garnet. Older, migmatitic dikes have tonalitic to trondhjemitic segregations spatially associated with garnet crystals. Where small, the segregations occupy tails or strain shadows on every garnet crystal. Where garnets and segregations are large, leucosomes form an interconnected network that extends into the host tonalite. Tonalitic pools, probably of dike origin, collect in boudin necks and fold hinges. The Chipman dikes are interpreted to have been emplaced, solidified, and partially melted during ductile shearing in the lowermost crust, perhaps near the base of an Archean island arc. They appear to offer an exceptional view of magma genesis where underplated mantle-derived mafic magmas provide not only heat but also a component of material to new felsic magmas. Deformation is essential to the process, allowing access of mafic magma into the lower crust and facilitating the segregation of the new felsic melts from their source rocks.

Introduction

The sources of felsic melts and the mechanisms of their segregation are issues of interest and controversy in the geologic literature [*Fyfe*, 1973; *Whitney*, 1988; *Brown*, 1994; *Sawyer*, 1994]. Felsic melts in arc settings are particularly important because of the role they play in the generation and stabilization of continental crust. Classical models have focused either on the evolution of felsic melts from mantle-derived mafic melts by fractional crystallization or on the anatexis of relatively felsic crust or sediments [see *Wyllie*, 1983]. More recently, workers have increasingly considered lower and middle crustal amphibolites as potential sources of felsic melts, particularly of tonalites and trondhjemites [*Percival*, 1983; *Beard and Lofgren*, 1991; *Rapp et al.*, 1991; *Rushmer*, 1991; *Winther and Newton*, 1991; *Wolf and Wyllie*, 1993, 1994]. Amphibolite melting in the lower crust may also provide a mechanism for producing garnet-bearing granulites as restites [*Fyfe*, 1970; *Wolf and Wyllie*, 1993]. Many previous studies have concentrated on compositional and petrological aspects of amphibolite anatexis. With few exceptions [*Percival*, 1983; *Sawyer*, 1991], exploration of tectonic aspects has been hindered by the rarity of structurally and tectonically constrained field occurrences.

The 3.2 Ga Chipman dike swarm of northern Saskatchewan is a superbly exposed natural example of deep crustal anatexis of amphibolites, involving segregations of tonalitic to trondhjemitic composition and a garnet-bearing restite. The dike swarm is interpreted to have formed near the base of an Archean magmatic arc. Mafic dikes were emplaced, deformed, and apparently partially melted during regional shearing [*Hanmer et al.*, 1994]. Deformation played a key role in all stages of evolution of the dike swarm, particularly in melt segregation and transport. The purpose of this paper

Paper number 95JB00760.
0148-0227/95/95JB-00760$05.00

is to describe the structural and tectonic setting of the migmatized dikes and to illustrate, on a variety of scales, the textures and fabrics which resulted from melting and melt segregation.

Geologic Background

The Striding-Athabasca mylonite zone [*Hanmer and Kopf*, 1993; *Hanmer et al.*, 1994; *Hanmer*, 1995] is a 400-km-long segment of the Snowbird tectonic zone, a regional northeast-trending linear anomaly in the horizontal gravity gradient map of the Canadian Shield [*Goodacre et al.*, 1987]. The Snowbird zone has been interpreted as the boundary, possibly a suture, between the Rae and Hearne Archean crustal provinces [*Hoffman*, 1988]. The Striding-Athabasca mylonite zone is particularly well exposed in the East Athabasca Mylonite Triangle (EAMT), at the eastern end of Lake Athabasca, Saskatchewan. There, a 40 km-wide zone of anastomosing granulite facies mylonites is separated from the Rae (northwest) and Hearne (southeast) province wall rocks by narrow greenschist facies shear zones (Figure 1) [*Hanmer*, 1995; *Hanmer et al.*, 1992, 1994].

The EAMT can be divided into three structural domains (Figure 1). All three have shallowly plunging, northeast trending mineral lineations. The southern domain, or upper deck, is dominated by mafic granulite and leucocratic gneiss [*Hanmer et al.*, 1994, 1995]. It has a shallow south dipping foliation and structurally overlies the other two domains. The northwestern domain contains felsic granitoids, tectonized migmatites, and a mafic plutonic complex. It has a vertical foliation and dextral strike-slip shear sense indicators. The southeastern domain is dominated by the Chipman tonalite and the Chipman dike swarm, the subject of this paper. It has a steeply dipping foliation but, in contrast to the northwestern domain, has sinistral strike-slip shear sense indicators.

Textural and microstructural evidence such as porphyroblast inclusion relationships and dynamic recrystallization in feldspars and pyroxenes indicates that all three domains were deformed under granulite facies conditions [*Hanmer et al.*, 1994]. In addition, parts of the upper deck experienced a phase of high-T, very high-P metamorphism (1000°C, >2.0 GPa) before decompression to granulite facies conditions [*Snoeyenbos and Williams*, 1994]. U-Pb geochronology indicates that the upper deck was emplaced, and the northwestern domain deformed, at 2.6 Ga, whereas most of the southeastern domain was deformed at approximately 3.2 Ga and reworked by the 2.6 Ga shearing [*Hanmer et al.*, 1994]. Our model for the tectonic history of the EAMT involves circa 3.2 Ga deformation and granulite facies metamorphism, possibly in an arc-related setting, and a second phase of granulite facies deformation and metamorphism at 2.6 Ga in an intracontinental setting [*Hanmer et al.*, 1994]. This second phase apparently juxtaposed and fused the three domains.

The southeastern, sinistral domain of the EAMT has two main lithotectonic components: the circa 3.2 Ga Chipman tonalite and the circa 2.6 Ga Fehr granite on the eastern edge of the domain. The Chipman tonalite hosts the Chipman mafic dike swarm and sheets of Chipman granite, both roughly coeval with the older phase of granulite facies shearing (circa 3.2 Ga) [*Hanmer et al.*, 1994].

The Chipman tonalite, from field observations, is a single lithologic/magmatic body, divisible into several structurally and metamorphically defined units. The central part is a hornblende tonalite with a coarse igneous texture and a weak foliation defined by aligned plagioclase and elliptical to banded inclusions of amphibolite and clinopyroxenite. The eastern portion is an annealed hornblende (± garnet) "straight gneiss" [e.g. *Myers*, 1978; *Hanmer*, 1988], with a sugary texture and a medium to fine grain size. In the western parts of the tonalite body, the primary fabrics and straight gneiss fabrics are locally overprinted by younger quartz- and feldspar-ribbon mylonites. All units of the Chipman tonalite contain inclusions of variably deformed anorthosite, layered amphibolite, orthopyroxenite, garnet clinopyroxenite, anthophyllite schist, and fresh peridotite. These may be fragments of a layered mafic complex that were dispersed throughout the tonalite [*Hanmer et al.*, 1994].

Two samples of the Chipman tonalite have been dated by U-Pb zircon analysis. A folded tonalitic straight gneiss has yielded a poorly constrained age of 3466 +327/-80 Ma, and a weakly foliated tonalite from the core of the Chipman tonalite body has yielded a poorly constrained age of 3149 ±100 Ma [*Hanmer et al.*, 1994]. All of the map units of the Chipman tonalite are truncated by discrete greenschist facies mylonites that define the eastern boundary of the EAMT.

Coarse, pinkish-red, equigranular leucogranites, informally termed the Chipman granite [*Hanmer et al.*, 1994], cut the Chipman tonalite. Although there are some relatively large bodies, most of the granite occurs as thin (0.1-1 m) veins. The veins are variably deformed, ranging from unfoliated and crosscutting with respect to the annealed straight gneiss fabric to foliated completely transposed components of the straight gneiss banding. The granite sheets are also syntectonic with respect to the Chipman dikes (see below), cutting across early members, but crosscut by later, less deformed or undeformed dikes. A 1 m-thick sheet of undeformed Chipman granite has been dated at 3127 ± 5 Ma. Because the granite sheets are contemporaneous with the (syntectonic and synmetamorphic) Chipman dikes, this date indicates the approximate time of granulite facies metamorphism, the time of mylonitization represented by the annealed straight gneisses, and the approximate time of emplacement of the Chipman dikes themselves [*Hanmer et al.*, 1994].

Chipman Dike Swarm

The Chipman tonalite is intruded by a swarm of mafic dikes, called the Chipman dikes by *Hanmer et al.* [1992, 1994] (Figure 2). These dikes were previously termed the Chipman sill swarm by *Macdonald* [1980], probably because they are generally concordant to the gneissic layering. The dikes range from 1 m to tens of meters in width. The main part of the swarm is hosted by the mylonitic straight gneisses in the eastern parts of the Chipman tonalite. There dikes can occupy between 60 and 100% of the outcrop in belts 1-2 km wide. Toward the west, they decrease in abundance, typically occurring as isolated dikes in tonalite-dominated outcrops. The main part of the dike swarm coincides with a positive gravity anomaly which may indicate the presence of similar material or even a mafic pluton at depth [*Hanmer et al.*, 1992, 1994].

The Chipman dikes were emplaced throughout a regional sinistral shearing and shortening event. The oldest dikes, based on crosscutting relations, define isoclinal folds, refolded folds, and sheath folds and display multiple foliations (including sinistral S and C foliations [*Berthe et al.*, 1979]), boudinage, and extreme thickness variation (Figure 2b). Some dikes can be traced along or across strike into zones of intense

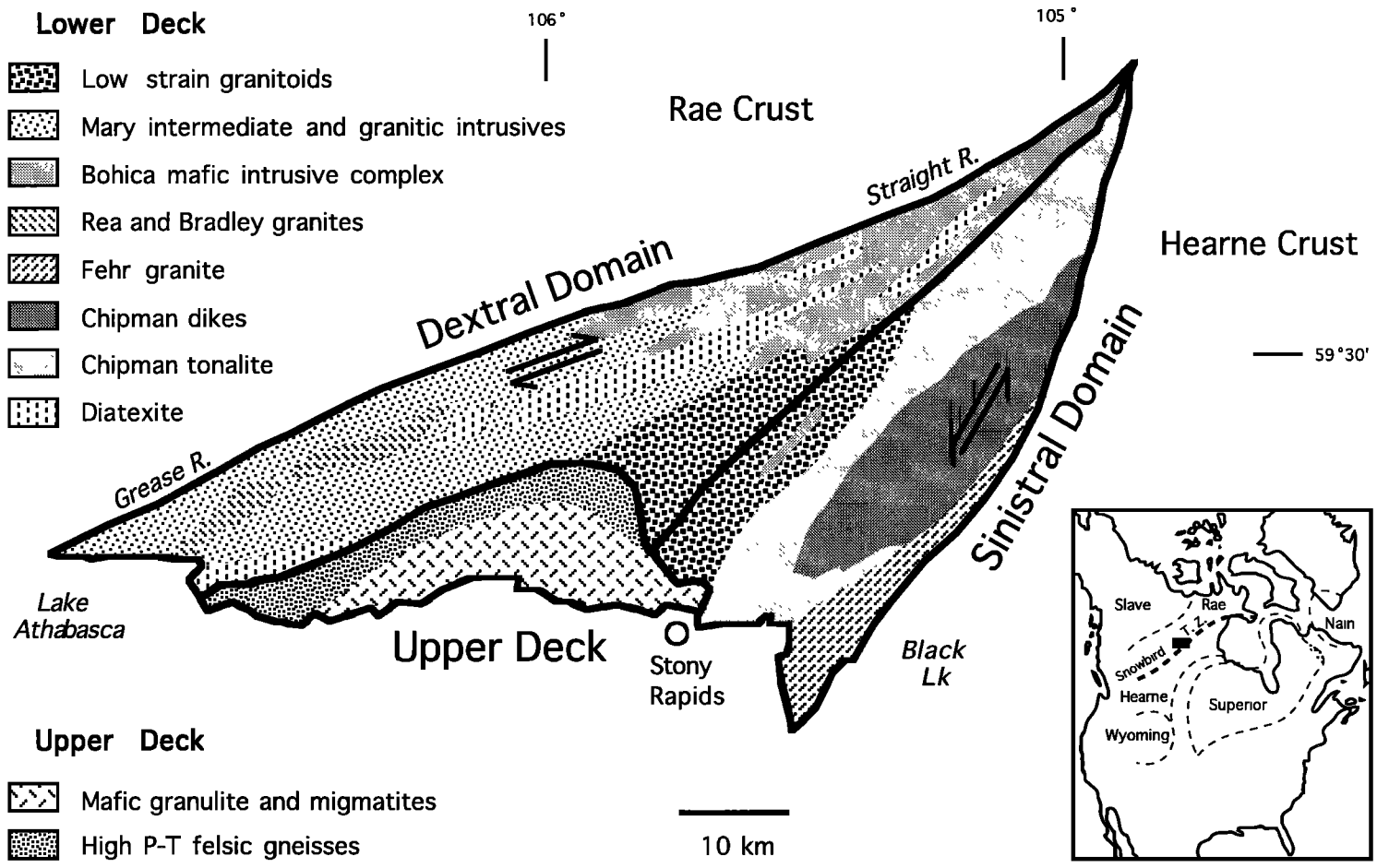

Figure 1. Geologic and structural elements of the East Athabasca Mylonite Triangle (EAMT), northern Saskatchewan. Inset shows location of EAMT along the Snowbird tectonic zone [*Hoffman*, 1988]. Geologic map modified from *Hanmer* [1995]. The Chipman dikes occur throughout the Chipman tonalite, but occur in greatest density toward the eastern side.

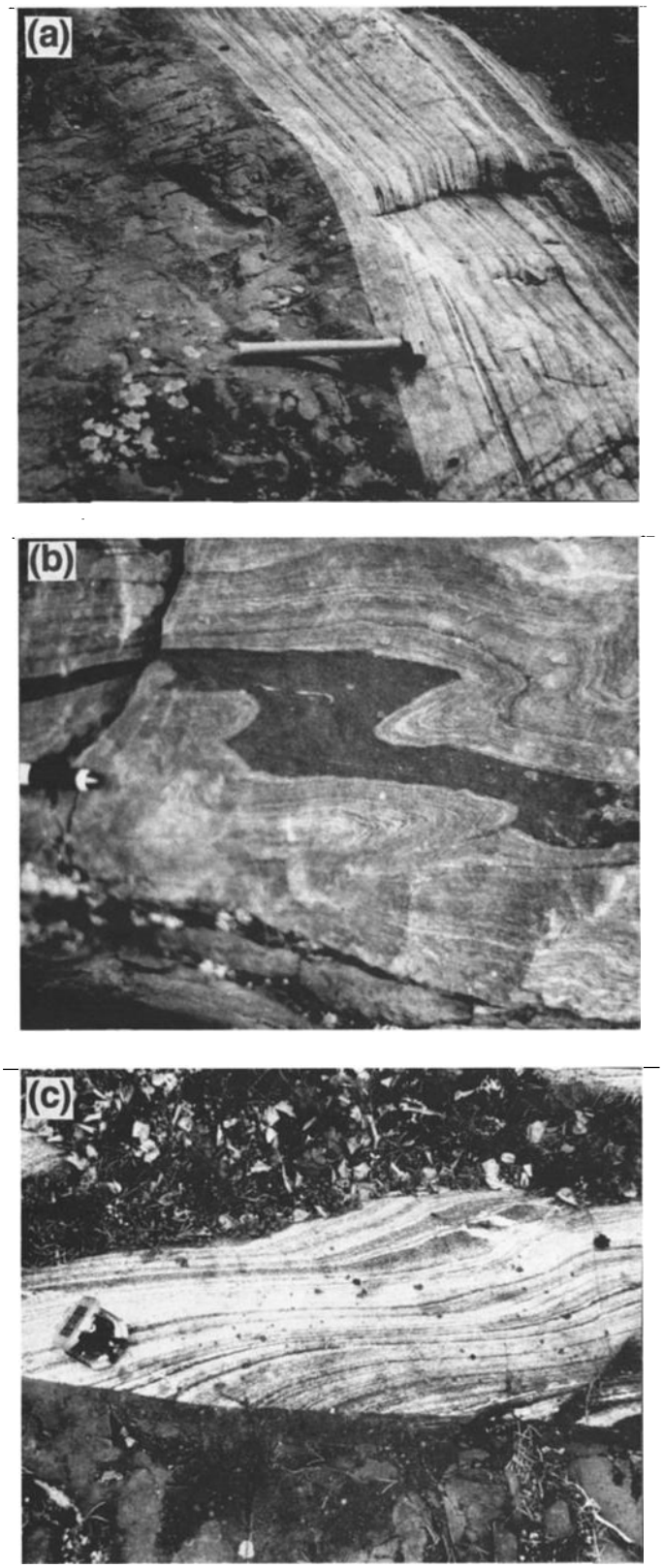

Figure 2. Timing relationships of Chipman dikes. (a) Typical exposure with concordant dike (left) and banded tonalite straight gneiss (right). A narrow, highly attenuated dike occurs to the right. (b) Deformed dike, first transposed into the mylonitic tonalite fabric and then both the dike and the tonalite were folded. (c) Relatively undeformed dike cleanly cuts all structures in the host tonalite.

shearing, locally to the point of becoming streaks or schlieren in the mylonitic tonalite. Younger dikes have sharp contacts that cleanly cut the older, more deformed dikes and the fabric in the mylonitic host tonalite (Figure 2c). Many of these younger dikes have randomly oriented wall rock inclusions, joint-controlled irregularities along their contacts, and delicate apophyses projecting into the wall rocks. Primary igneous textures including chilled margins and concentrations of plagioclase phenocrysts in the centers of dikes are also common, especially in the least deformed dikes.

Kinematics of Emplacement

The emplacement of mafic dike swarms is commonly interpreted in terms of extensional tectonics [e.g., *Wolf and Saleeby*, 1992]. The Chipman dikes, however, were emplaced during sinistral, strike-slip, ductile shearing. Most are strongly deformed and nearly concordant to the fabric of the host tonalite. However, the least deformed examples preserve a kinematically significant geometry. The great majority of undeformed dikes occur in orientations 15-25° counterclockwise from the fabric of the tonalitic straight gneiss; the rest either are concordant to the fabric or make a clockwise angle of 15-20° [*Hanmer*, 1995]. Asymmetrical apophyses systematically indicate that the counterclockwise dikes were emplaced into left-stepping (sinistral) fracture arrays. Most of the clockwise dikes which preserve asymmetrical apophyses were emplaced into right-stepping (dextral) fracture arrays, but at least two dikes fill left-stepping (sinistral) arrays.

Hanmer [1995] suggested that the fracture arrays into which the Chipman dikes were emplaced correspond to the Reidel R and P fracture planes, predicted for sinistral shear [e.g., *Logan*, 1979; *Gamond*, 1983]. Fracturing of the otherwise plastic gneisses probably occurred during transient excursions into the brittle deformation field [*Sibson*, 1980], possibly enhanced by the effects of the forcible emplacement of the pressurized mafic magma. The symmetry of the dikes with respect to the straight gneiss fabric and the opposing sense of shear recognized on some of the clockwise and counterclockwise dikes suggest a component of shortening normal to the flow plane. Postemplacement shortening and sinistral shearing resulted in boudinage and synthetic rotation of the clockwise dikes into the bulk flow plane; the counterclockwise dikes rotated antithetically (back rotated) toward the same final orientation [e.g., *Hanmer and Passchier*, 1991].

Metamorphic Assemblages and Textures

Mineral assemblages and textures in the Chipman dikes are variable from dike to dike and to a lesser degree within individual dikes. Because crosscutting relationships are commonly preserved, the dikes and the textures can be placed into a relative age sequence. All of the dikes contain fine- to medium-grained recrystallized hornblende and plagioclase with varying amounts of fine grained clinopyroxene. Garnet is present in virtually all dikes, but its size and abundance increase in progressively older, more deformed dikes. Garnet-rich dikes contain the widest variety of textures; some of the oldest and most deformed have huge euhedral garnet crystals, up to 10 cm in diameter.

The Chipman dikes can be divided into two broad textural and mineralogical groups (Figures 3 and 4), (1) migmatitic dikes in which garnet crystals are associated with distinctive quartz + plagioclase leucocratic segregations (Figures 3a and 4a), and (2) nonmigmatitic dikes in which fine-grained garnet and clinopyroxene occur in spherical concentrations with

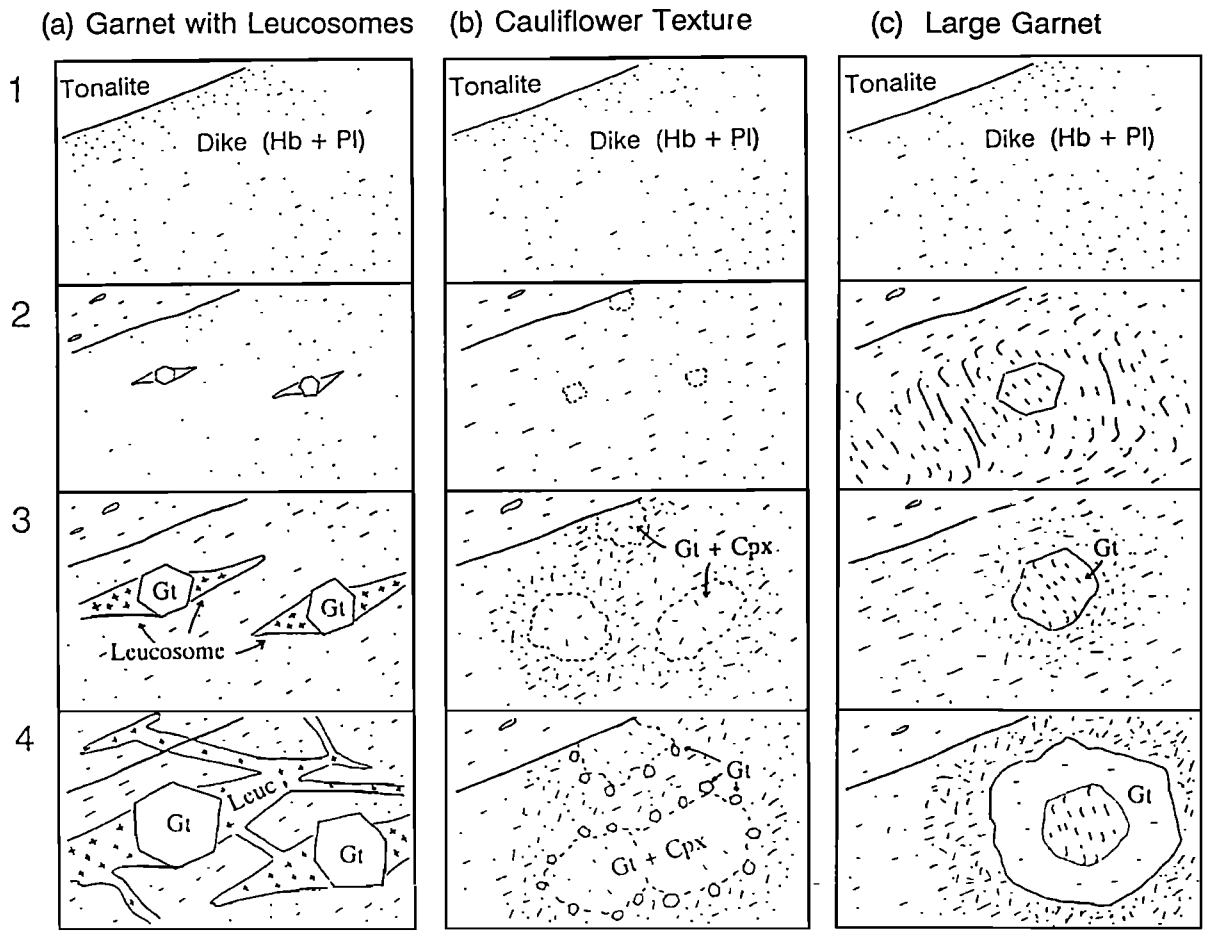

Figure 3. Common metamorphic reaction textures in Chipman dikes. Four progressive stages are shown for each reaction, numbered 1-4. (a) Euhedral garnet crystals grow with leucocratic segregations, interpreted to be tonalitic partial melt. (b) Garnet-clinopyroxene-ilmenite (Grt-Cpx-Ilm) assemblages (without leucosomes) in spherical domains resembling cauliflowers, typically decorated with a necklace of euhedral garnet crystals. (c) Extremely large garnet without clinopyroxene or melt. Hornblende concentration increases in proportion to garnet volume.

scalloped, cauliflower-shaped boundaries in a medium to course grained, hornblende + plagioclase matrix (Figures 3b and 4b). A second, less common, non-migmatitic texture involves extremely large garnets surrounded by hornblende-rich matrix which grades into typical hornblende+plagioclase matrix (Figures 3c and 4c). No consistent age relationships have been observed among these textural varieties, and in some cases, a single dike hosts two or more of the reaction textures. These observations, plus the similarity of their interpreted P-T conditions (see below), suggest that local compositional variations, particularly involving H_2O and SiO_2, may have controlled the reactions and textures.

The leucosome-bearing Chipman dikes are the principal focus of this paper; leucosome-absent textures and equilibria will be discussed in a separate contribution. Although nongenetic, migmatite terminology is used throughout the following descriptions, the textures strongly suggest that the leucosome results from in situ partial melting. The implications of this interpretation are presented in the discussion section (below).

Migmatite Styles and Textures

The matrix of all migmatized dikes consists of hornblende and plagioclase with variable amounts of quartz, titanite, biotite, and ilmenite. Clinopyroxene is rare or absent. Hornblende and plagioclase are medium grained in all dikes regardless of degree of deformation or metamorphism. Hornblende typically defines a foliation and mineral lineation. The foliation is generally parallel to the large-scale sinistral flow plane, although local S and C foliations are also common. Some hornblende crystals contain inclusion trails of fine-grained aligned quartz and plagioclase, suggesting that a foliation existed at the time of hornblende growth and thus that these amphiboles cannot be original igneous crystals. Instead, they are new crystals that were produced during deformation and dynamic recrystallization.

Garnet is ubiquitous in the migmatized dikes. In any one dike, garnet crystals tend to be relatively uniform in size, but from dike to dike, they range from less than 1 mm to more than 5 cm. Younger, less deformed dikes tend to host small garnets; older, more deformed dikes have the largest garnets. Some large garnet crystals contain inclusion trails consisting of fine-grained, aligned quartz, plagioclase, hornblende, and rarely biotite. The trails commonly have a sigmoid geometry suggesting that the garnets have either rotated during growth or they have overgrown small-scale folds. The fact that these aligned inclusions tend to be finer in size and less equant than the matrix minerals is additional evidence that the present

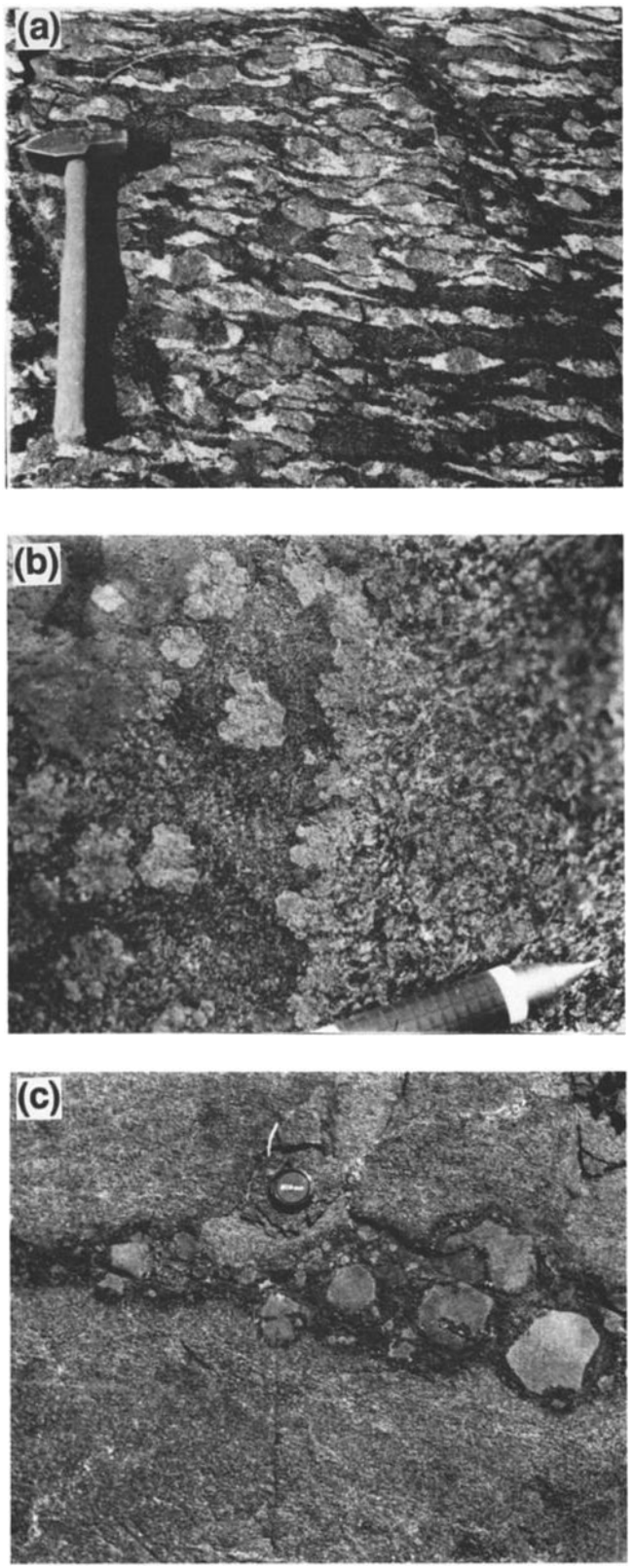

Figure 4. Examples of three common reaction textures from Figure 4. All three textures/reactions occur in medium-grained amphibolite dikes: (a) leucocratic segregations associated with large (2-3 cm) garnet, (b) small Grt-Cpx cauliflowers surrounded by euhedral garnet crystals (left); homogeneous garnet granulite (right); (c) large euhedral garnets with hornblende-rich envelope.

matrix phases have experienced a significant amount of coarsening and recrystallization after the time of anatexis.

Leucosomes. Leucosomes occur in two main textural varieties: (1) associated with garnet crystals and (2) as independent pods and veins (here termed discrete leucosomes). In dikes with relatively small garnets (<2 cm), virtually all leucosomes occur adjacent to garnets, with sizes directly proportional to that of the garnet crystals, i.e., small garnets have small segregations (Figure 5a); large garnets have larger segregations (Figure 5b). The size proportionality remains consistent over the entire area of dike exposure. Where garnets are relatively large (> 2 cm), "discrete" leucosome segregations are present as pods and veins. Garnets near these larger segregations commonly have disproportionately small or nonexistent segregations (see below).

The leucosomes contain quartz (20-30%) and plagioclase (65-75%), with variable but small amounts of hornblende and potassium feldspar. Because many segregations contain no mafic phases at all, hornblende, where present, is believed to represent disaggregated crystals from the matrix rather than a crystallization product from the leucosomes. The segregations are undeformed to moderately deformed. Feldspar crystals are large (2-4 mm) with grain boundaries that range from straight (rather rare) to irregularly sutured. The crystals have a slight dimensional preferred orientation parallel to the matrix fabric, perhaps indicating some flow in a liquid state. Most of the feldspars have albite twins, whereas matrix feldspars are generally untwinned. In the most deformed segregations, subtle subgrains and neocrystals are locally present on grain boundaries. Quartz is generally finer grained than feldspar and tends to fill spaces between the feldspar crystals, although some larger vermiform grains are also present. The quartz shows more evidence of solid state deformation than feldspar; subgrains and lamellae are common. Toward the outer parts of the segregations, quartz grains are more equant and have smooth 120° triple junctions.

Leucosomes are everywhere structurally controlled. Most commonly, the segregations occur in strain shadows adjacent to the garnet crystals (Figure 5). Two triangular-shaped segregations extend away from garnets as tails (Figures 5a, 5b, and 5c), similar to winged porphyroclasts [*Hanmer and Passchier*, 1991], or sigma tails [*Passchier and Simpson*, 1986]. The tails typically step up from the right to the left side of the central garnet, indicating sinistral shear (Figure 5c). Some migmatized dikes display classic S and C foliations [*Berthe et al.*, 1979] (Figure 5d). The dike-parallel foliation and tonalite fabric define the shear plane (C), while the leucosomes and a subtle, second fabric in the amphibolite define the S planes. The S planes are oriented at an angle of approximately 30-40° to the dike margin, but near the margin, they curve into the main foliation. Where dikes are folded, leucocratic segregations associated with garnet commonly define an axial plane fabric (Figure 5e). In some dikes, segregations that developed along the dike-parallel fabric have partially transposed into the axial plane orientation.

Some migmatitic dikes display a subtle to marked internal layering, generally parallel to the dike margins (see Figures 5a, 5b, and 5e). This layering involves planar domains with differing abundances and sizes of garnet+leucosome structures (i.e., domains in which the leucosome-forming process has proceeded to a greater or lesser extent). Dikes only 1 or 2 m wide can have as many as 10 internal layers. The boundaries between domains are gradational and are quite

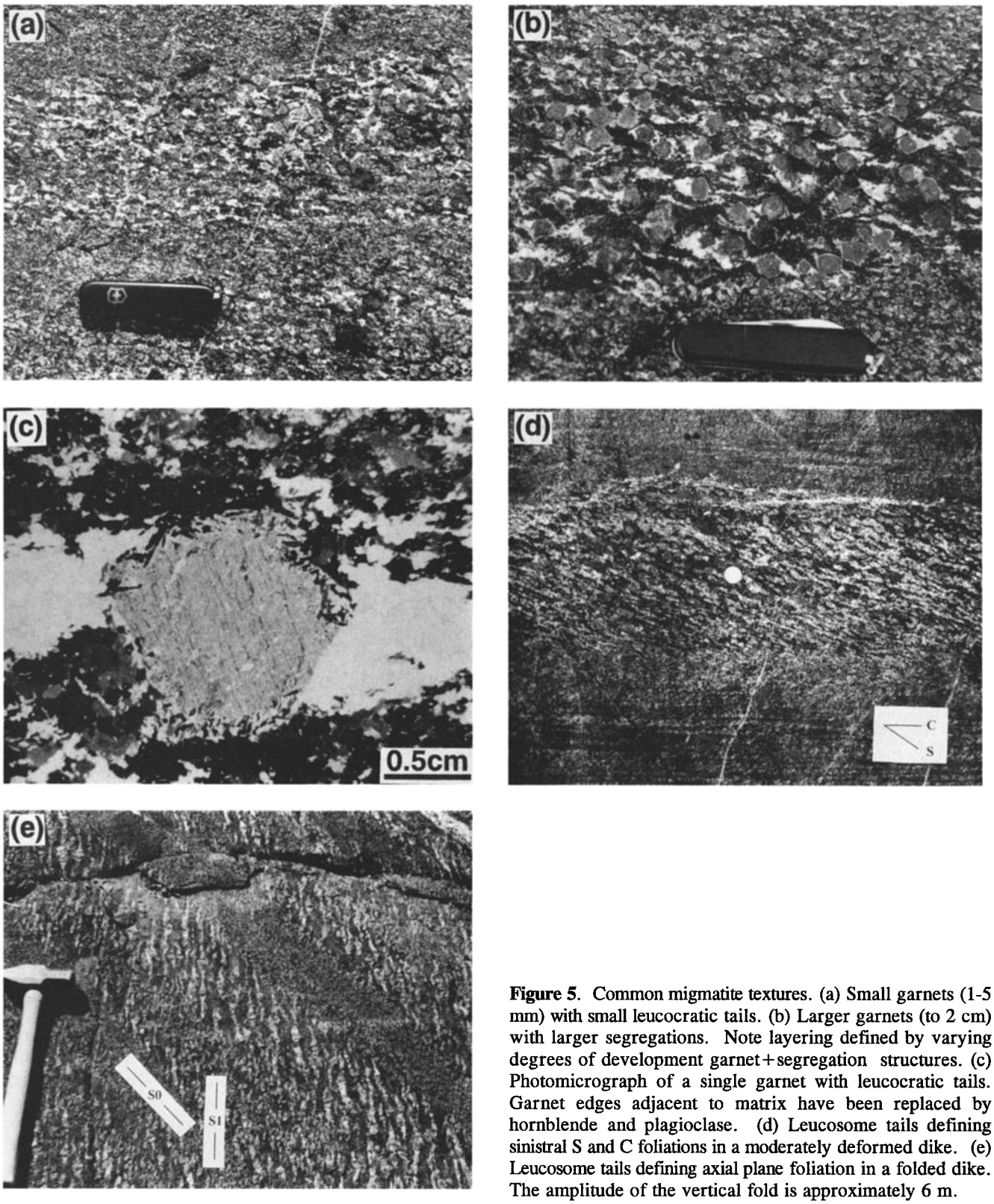

Figure 5. Common migmatite textures. (a) Small garnets (1-5 mm) with small leucocratic tails. (b) Larger garnets (to 2 cm) with larger segregations. Note layering defined by varying degrees of development garnet+segregation structures. (c) Photomicrograph of a single garnet with leucocratic tails. Garnet edges adjacent to matrix have been replaced by hornblende and plagioclase. (d) Leucosome tails defining sinistral S and C foliations in a moderately deformed dike. (e) Leucosome tails defining axial plane foliation in a folded dike. The amplitude of the vertical fold is approximately 6 m.

distinct from the sharp boundaries observed in composite dikes. The layering may reflect primary compositional variation or flow-related variation across the dikes that has been enhanced by strain heterogeneity and fluid gradients related to dehydration and rehydration during metamorphism.

Discrete leucosomes. Migmatized dikes with relatively large garnets typically contain discrete leucocratic segregations that are not associated with garnet crystals (Figure 6). It is important to note that these segregations are generally not present in dikes with smaller garnet + leucosome structures, and even beyond the point where discrete leucosomes appear, the total volume of leucocratic material increases in proportion to garnet size. Many dikes with garnets of the order of 2-5 cm host irregular-shaped pods of leucosome material 5-10

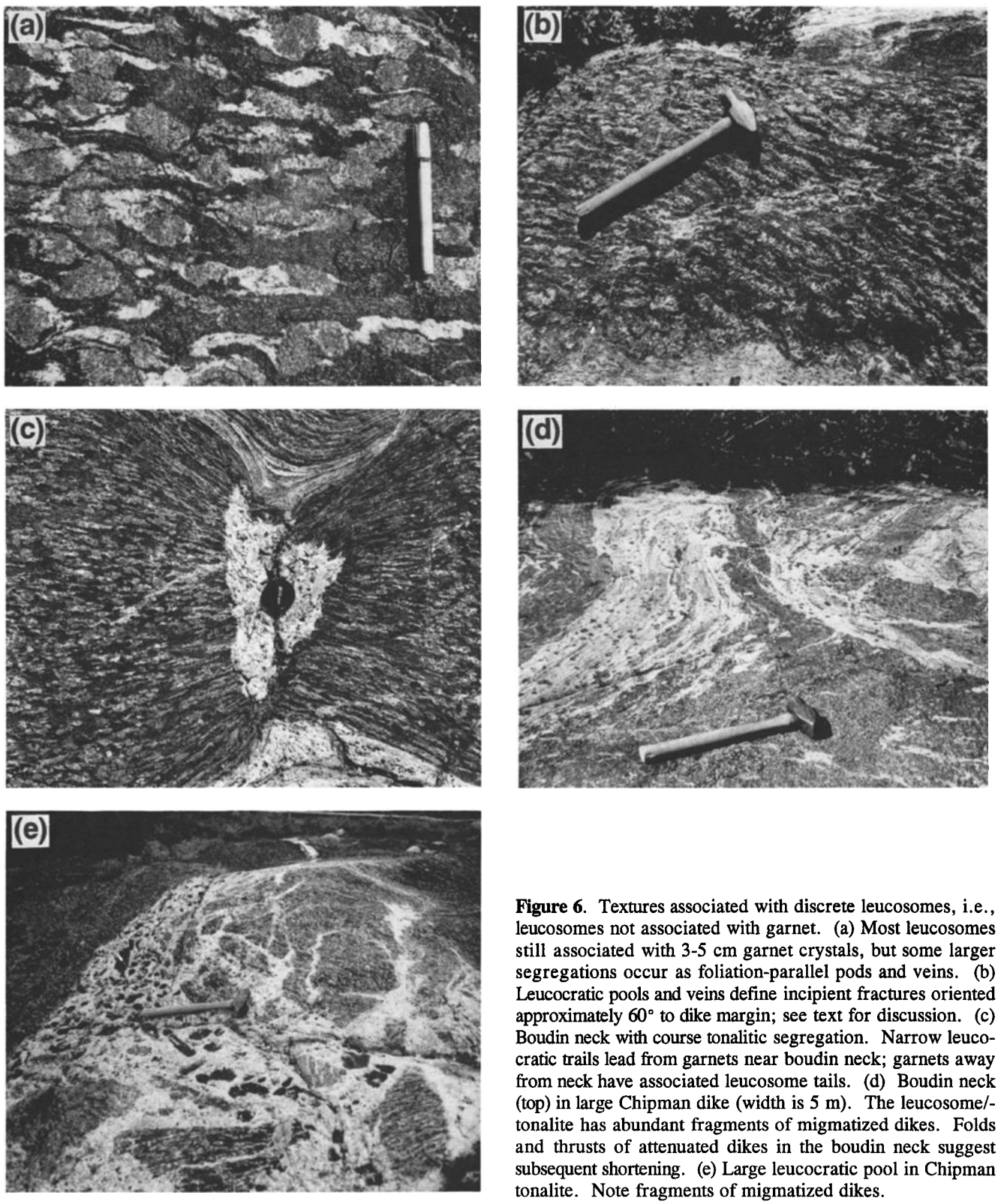

Figure 6. Textures associated with discrete leucosomes, i.e., leucosomes not associated with garnet. (a) Most leucosomes still associated with 3-5 cm garnet crystals, but some larger segregations occur as foliation-parallel pods and veins. (b) Leucocratic pools and veins define incipient fractures oriented approximately 60° to dike margin; see text for discussion. (c) Boudin neck with course tonalitic segregation. Narrow leucocratic trails lead from garnets near boudin neck; garnets away from neck have associated leucosome tails. (d) Boudin neck (top) in large Chipman dike (width is 5 m). The leucosome/-tonalite has abundant fragments of migmatized dikes. Folds and thrusts of attenuated dikes in the boudin neck suggest subsequent shortening. (e) Large leucocratic pool in Chipman tonalite. Note fragments of migmatized dikes.

cm in diameter (Figures 6a and 6b). These pods or pools are 5-10 times larger than the largest garnet tail, and are interpreted to have accumulated from a number of garnets. Locally, narrow leucocratic trails or pathways can be seen leading from nearby garnets that are missing one or both of their leucocratic tails. Other dikes contain leucocratic material in veins or gashes. These veins are commonly oriented at approximately 60° to the dike walls and typically do not extend into the host tonalite (Figure 6b). They may fill extensional fractures developed during the early stages of boudinage.

Some dikes display well-developed boudinage with vertical boudin necks (i.e., subhorizontal extension). The boudin necks are invariably filled with leucocratic segregations

(Figures 6c and 6d). In the best examples, trails or narrow veins can be seen leading from garnet crystals in the dike to the boudin neck. Leucocratic tails are absent from the garnets connected to these trails, suggesting that the segregations have been mobilized into the boudin necks. In the most advanced stages of leucosome formation, dikes are cut by numerous leucocratic veins that do extend into the host tonalite. In addition, pools and veins of tonalite, preserving a complete range of deformation states and interpreted to be of dike origin, occur within the mylonitic Chipman tonalite. The largest pools can be meters to tens of meters across and typically contain rafts of partially digested dike material, with leucocratic segregation still evident (Figure 6e).

One observation suggests that the segregation forming process can be cyclical in the dikes. Garnet crystals nearest to the boudin necks and garnets in xenoliths in large tonalite pools are partially to completely replaced by hornblende and plagioclase (Figure 6c). Some of the reequilibrated domains contain new euhedral garnet crystals with new small leucocratic tails, suggesting that a second stage of migmatization has occurred after one complete cycle of garnet growth, leucosome segregation, and garnet replacement.

Figure 7 is a sketch of one well-exposed example of the spatial relationships of dikes of several ages. The dikes are numbered from oldest to youngest. Dike 1 is highly dismembered with large garnets and only remnants of leucocratic segregations. Inclusion trails in the garnets suggest that they predate the major fold in the outcrop. They are straight or weakly curved and truncated by the dominant axial plane foliation. Dike 2 has very large garnets and large leucocratic

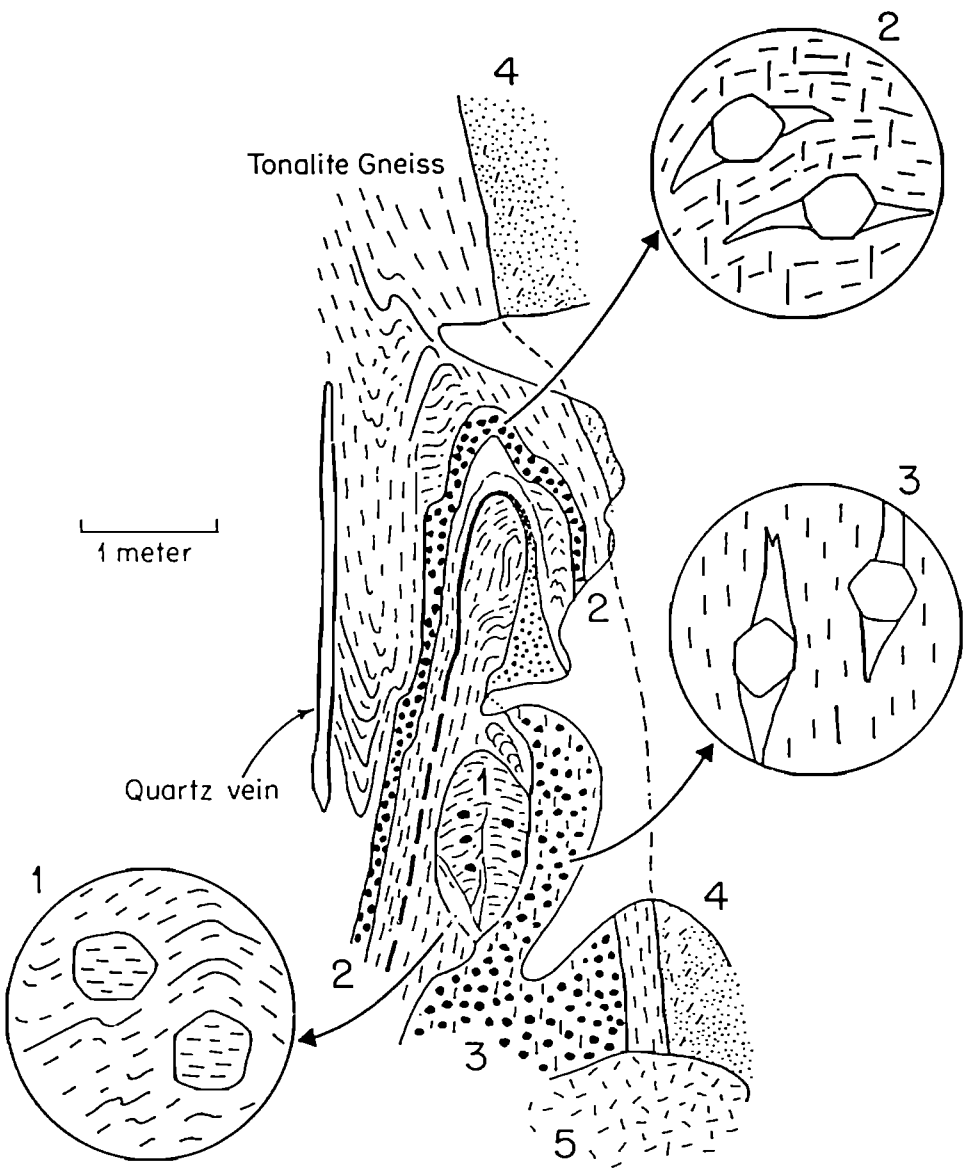

Figure 7. Outcrop sketch illustrating timing of dike emplacement, metamorphism, and deformation. Dikes are numbered from oldest to youngest. Dike 1 is highly dismembered with large garnets and remnants of leucocratic segregations. Inclusion trails are straight. Leucocratic tails in dike 2 are folded around the fold, and thus they existed before or early during folding. Leucocratic tails in dike 3 define the axial surface of the fold, so migmatization occurred during folding. Dike 4 cross-cuts the axial fabric, and thus is younger than dike 3. Dike 5 is a coarse-grained leucocratic segregation that cuts all of the visible fabrics. See text for discussion.

tails that are folded around the outcrop scale fold. These tails probably existed before folding. Dike 3 has slightly smaller garnets and tails, and these tails define the axial surface of the outcrop-scale fold. Migmatization of this dike apparently occurred during folding or tightening of the fold. Dike 4 crosscuts the axial fabric and thus is younger than dike 3. It contains only submillimeter-sized garnets, each with small leucocratic tails. Dike 5 is a coarse grained leucocratic segregation that cuts all of the visible fabrics.

These relationships illustrate several important aspects of dike emplacement, deformation, and metamorphism that are indicated in most exposures but more clearly demonstrated here. First, the Chipman dikes were emplaced syntectonically and synmetamorphically at granulite facies. New dikes were emplaced, while older dikes were undergoing progressive sinistral shearing and partial melting. Because the new dikes were emplaced during garnet growth, determined to be at 1.0 GPa, the dikes were emplaced at depths of the order of 30 km. Second, the dikes were emplaced with a significant amount of amphibole (i.e., with significant H_2O); they were apparently not emplaced as dry basalt or gabbro and subsequently hydrated to the amphibolite assemblages.

Major and Trace Element Compositions

Major element analyses. Whole rock geochemical analyses of nine separate Chipman dikes and four leucocratic segregations are presented in Table 1. For comparison, the starting amphibolite composition from partial melting experiments of *Wolf and Wyllie* [1993, 1994] are also included (see below for discussion). The Chipman dikes are relatively uniform in composition regardless of their reaction textures or metamorphic history (Figure 8a). On the basis of major elements they are quartz tholeiites, and all lie near the plane of silica saturation. Four of the dikes have normative olivine and five have normative quartz. All four dikes with normative olivine are nonmigmatized, and dike M2432C, with the greatest amount of normative quartz, has experienced the greatest amount of migmatization. This supports the suggestion that bulk composition, particularly the activity of SiO_2, has played a role in controlling the reaction history of the dikes.

Trace element profiles are relatively flat at approximately 10-40 times chondrites, although some dikes are slightly depleted in incompatible trace elements (Figure 8b). Overall, the signatures are typical of mid-ocean ridge basalts (MORBs) or perhaps some island arc tholeiites [*Wilson*, 1989, p.142]. Discriminant diagrams based on major and minor elements generally indicate that the Chipman dikes resemble island arc tholeiites. This is compatible with the MORB character of the trace elements, especially considering that these dikes could have been emplaced near the Moho and thus may have had little interaction with the crust. It is important to note that none of the dikes analyzed to date contain discrete segregations (i.e., leucosomes not associated with garnet) or show evidence for separation of leucosomes from the dikes, so the major and trace elements do not reflect enrichments and depletions due to the extraction of leucocratic material.

Table 1 includes five analyses of leucosome compositions. M61-P is an average of more than 300 broad-beam, microprobe analyses from a single leucocratic garnet tail (Pl 70% and Qtz 30%) from locality M61. The remaining compositions were determined by XRF analysis of segregations that were sawn from their host dikes and hand picked. M61 is a second sample from locality M61; several leucocratic tails were combined and analyzed. C26 is a separate locality, several kilometers from M61, with well-formed 1-cm-long leucocratic tails. C24-N and C24-H are from a small, discrete leucocratic segregation completely contained in its host dike. Narrow leucosome trails connect the segregation to large (>3 cm) garnet crystals without leucocratic tails. C24-H includes a small amount of fine hornblende, whereas analysis C24-N contains no visible hornblende. In terms of major elements, all of the leucosomes analyzed to date are either tonalites or trondhjemites (Figure 8c), but they are distinctly deficient in mafic components reflecting the general lack of mafic phases. For comparison, S152A is a sample of mylonitic Chipman tonalite. Its composition is extremely similar to that of the leucosomes, but it is richer in iron and magnesium, reflecting a significant percentage of hornblende.

The leucosomes are generally poor in most trace elements, except Ba, Ce, and Sr, compared to the whole dike analyses and to the Chipman tonalite. This trace element behavior is similar to that of leucosomes described by *Sawyer* [1991]. Sawyer concluded that trace element rich phases such as zircon and apatite are preferentially retained in the mafic rocks during leucosome formation and thus are deficient in the leucosomes. He noted that the concentration of Ba depends on the presence or absence of biotite in the host rocks. The Chipman dikes generally contain a only small amount of biotite perhaps explaining why the leucosomes are not particularly enriched or depleted in Ba. It is perhaps no surprise that leucosome C24-H falls between C24-N and Chipman tonalite in virtually all trace elements. Many of the compositional differences between the leucosome material and the Chipman tonalite can be accounted for by hornblende in the Chipman tonalite.

Mineral analyses. Table 2 summarizes mineral compositions for the major phases from a single migmatized Chipman dike (M-61) for which whole rock analyses were also carried out (Table 1). Garnet, 1-1.5 cm in diameter, is essentially an almandine-grossular mix. Most of the larger garnet crystals are zoned from core to rim (Figure 8d). Spessartine decreases and pyrope, almandine, and grossular increase from core to rim. The Mg number, Mg/(Mg+Fe), also increases slightly from core to rim, regardless of the adjacent matrix mineralogy. Against matrix minerals, garnet shows a slight decrease in Mg number at its edge. Against melt, it shows essentially no reversal in Mg number. The zoning is interpreted to reflect prograde garnet growth with a small amount of retrograde diffusional reequilibration.

Hornblende compositions are generally uniform across a single crystal and across a thin section. Ferric iron contents of approximately 5 wt % calculated according to method IV of *Robinson et al.* [1982] are typical of all of the migmatitic dikes. Hornblende is ferro-pargasite according to the classification of *Leake* [1978], and it ranges from hornblende to tschermakitic hornblende according to *Giret et al.* [1980]. Some hornblende crystals have narrow rims that are slightly enriched in Mg/(Mg+Fe) compared to the uniform cores. These compositions probably reflect a small amount of diffusional reequilibration, presumably with garnet, after the metamorphic peak.

Plagioclase is typically near An_{30}, and most crystals are unzoned. Some plagioclase displays narrow An-richer rims (An_{35}-An_{40}), which are interpreted to reflect a small amount of late stage decompression and garnet resorption. Plagioclase in leucosomes is more albitic than matrix plagioclase, and is typically unzoned. The general lack of zoning in plagioclase

Table 1a. Whole Rock Analyses of Chipman Dikes

	Dikes With No Leucosomes			Dikes With Small Leucosomes			Dikes With Large Leucosomes			
	M112-D	W2-36A	M112-2	W2-41	M2479B	M2432B	W2-26	M2432C	M110	W&W94
					Major Elements, wt%					
SiO_2	49.69	49.06	51.63	49.26	49.61	43.23	51.52	50.97	50.10	48.50
TiO_2	1.31	1.83	1.46	3.09	0.60	1.19	1.78	1.68	1.32	0.40
Al_2O_3	13.54	12.85	14.28	12.97	16.33	16.91	13.10	13.22	13.50	14.40
Fe_2O_3	15.34	18.28	14.17	16.95	11.80	16.86	16.05	17.52	15.90	9.44
MnO	0.21	0.29	0.22	0.22	0.19	0.25	0.22	0.34	0.29	0.20
MgO	6.20	5.57	5.65	5.13	8.48	9.32	4.72	5.12	5.99	10.80
CaO	9.90	10.09	9.52	9.16	10.87	11.43	8.88	9.34	10.10	14.80
Na_2O	2.65	1.85	2.53	2.46	2.11	1.02	2.61	1.27	1.70	1.70
K_2O	0.75	0.32	0.62	0.49	0.38	0.18	0.91	0.22	0.65	0.20
P_2O_5	0.11	0.16	0.14	0.34	0.05	0.13	0.18	0.16	0.13	0.00
Total	99.69	100.30	100.22	100.06	100.40	100.53	99.97	99.83	99.68	100.44
					CIPW Norms (plus small amounts of Ilm, Mag, Or)					
Ab	22.4	15.6	21.4	20.8	17.8	8.6	22.1	10.7	14.38	14.37
An	22.8	25.8	25.8	22.9	34.0	41.0	21.4	29.7	27.29	31.04
Or	0.0	0.0	0.0	0.0	0.0	0.0	0.0	0.0	0.00	0.00
Di	21.2	19.4	17.0	16.9	16.0	12.2	18.0	13.0	18.56	34.12
Hy	19.0	22.8	20.0	19.2	20.4	11.3	18.8	24.3	31.96	0.83
Ol	1.4	0.0	0.0	0.0	4.3	17.5	0.0	0.0	0.85	14.64
Qtz	0.0	4.1	4.0	4.4	0.0	0.0	4.7	10.7	0.00	0.00
					Trace Elements (ppm)					
Nb	4	7	8	13	2	9	12	9	10	
Zr	77	117	115	212	47	75	139	109	27	
Sr	140	118	172	136	160	267	226	112	129	
Ce	13	21	30	37	10	10	46	18	23	
Ba	68	60	184	56	72	15	230	27	106	
La	5	4	12	13	9	5	20	6	10	
Y	28	33	25	53	13	32	25	31	24	
U	1	1	1	1	0	1	1	0	0	
Rb	8	6	21	7	7	2	20	2	13	
Th	0	0	2	1	0	0	2	1	1	
Pb	2	2	5	3	3	3	7	4	2	

M112-D (Hbl-Pl-Qtz), coarse amphibolite, no melting; W2-36A (Grt-Cpx-Hbl-Pl-Qtz), cauliflower texture, no melting; M112-2 (Grt-Cpx-Pl-Qtz +/- Hbl), coarse garnet granulite, no melting; W2-41 (Grt-Cpx-Hbl-Pl-Qtz), cauliflower texture, no melting; M2479B (Grt-Cpx-Pl-Qtz +/- Hbl), coarse garnet granulite, minor melting; M2432B (Grt-Hbl-Pl-Qtz), large garnet (> 4 cm) in hornblende-rich matrix, minor melting; W2-26 (Grt-Hbl-Pl-Qtz-Leucosome), garnets (<5 mm) with leucosome tails; M2432C, M110 (Grt-Hbl-Ol-Qtz-Leucosome-Bt), large garnets (>1 cm) with large leucosome tails; W&W94, amphibolite used in melting experiments of *Wolf and Wyllie* [1994]. Mineral abbreviations after *Kretz* [1983].

and hornblende is taken as additional evidence that dynamic recrystallization was occurring during metamorphism and migmatization. During migmatization, compositional homogeneity was apparently maintained by strain-induced grain boundary migration and recrystallization. A similar explanation may apply to hornblende, although intragranular diffusion may also have contributed to the homogeneity. After the thermal event, diffusion was apparently too slow to allow significant reequilibration of matrix and segregation plagioclase compositions. This probably reflects the relatively slow intracrystalline diffusion in the absence of deformationally induced recrystallization, possibly combined with the loss of an intergranular exchange medium such as fluid or melt [*Pattison and Begin*, 1994].

Biotite generally occurs near and within garnet edges. The fact that the biotite occurs in the garnet suggests that it was present at the peak of metamorphism. However, its present composition is believed to reflect diffusional exchange with garnet during the cooling history. This is indicated by the generally lower temperatures obtained from garnet-biotite thermometry compared to garnet-hornblende equilibrium (see below).

Table 1b. Whole Rock Analyses of Migmatites

	M61P	M61	C26	C24N	C24H	Chipman Tonalite S152A
			Major Elements, wt%			
SiO_2	70.58	77.07	74.17	73.01	71.39	68.20
TiO_2	0.00	0.01	0.03	0.01	0.18	0.52
Al_2O_3	16.70	12.91	15.42	16.02	15.67	14.30
Fe_2O_3	0.38	1.0	0.49	0.31	1.77	6.10
MnO	0.00	0.03	0.01	0.01	0.02	0.05
MgO	0.00	0.20	0.18	0.02	0.44	1.43
CaO	3.14	3.59	3.20	3.89	4.09	2.87
Na_2O	5.54	3.36	4.59	5.07	4.77	4.40
K_2O	1.54	0.71	1.02	0.21	0.49	1.46
P_2O_5	NA	0.03	0.01	0.03	0.07	0.15
Total	97.88	99.02	99.11	98.57	98.90	99.48
			CIPW Norms (Plus Small Amounts of Ilm, Mag, Or)			
Ab	47.90	28.42	38.83	42.94	40.36	37.23
An	15.90	17.67	15.89	19.11	19.85	13.26
Or	9.30	4.17	6.02	1.22	2.91	8.63
Di	0.00	0.00	0.00	0.00	0.00	0.00
Hy	0.00	2.19	1.33	0.62	4.08	14.00
Ol	0.00	0.00	0.00	0.00	0.00	0.00
Qtz	26.30	46.13	36.05	34.16	31.16	24.41
			Trace Elements (ppm)			
Nb		1	0	0	3	7
Zr		3	0	17	32	169
Sr		484	413	571	536	415
Ce		7	10	38	28	59
Ba		95	95	82	145	205
La		4	3	18	145	205
Ni		5	7	0	0	NA
Cr		3	2	4	5	NA
Zn		5	5	9	24	NA
V		6	9	1	14	NA

M61P, same as M61: analysis represents average of 300 microprobe analyses; M61, leucosomes adjacent to ~1 cm garnet; C26, leucosomes adjacent to ~1 cm garnets; C24N, clean leucosome from small pod, trails connect to nearby garnets; C24H, same as C24N but contains ~2% dispersed hornblende; S152A, annealed Chipman tonalite mylonite gneiss.

Thermobarometry. Pressure and temperature estimates have been obtained from migmatitic and nonmigmatitic dikes using a variety of calibrated equilibria. Garnet-hornblende thermometry [*Graham and Powell*, 1984] and garnet-hornblende-plagioclase barometry [*Kohn and Spear*, 1989] have been found to be most useful because appropriate assemblages are present in virtually all dikes. Clinopyroxene is only locally present in migmatitic dikes, and biotite compositions have apparently been modified by late stage reequilibration, so equilibria involving these phases are less widely applicable. All of the dikes investigated to date yield temperatures of the order of 750-850°C and pressures of approximately 1.0 Gpa, regardless of relative age or degree of deformation. Figure 9 shows P-T estimates based on garnet-hornblende-plagioclase-quartz thermobarometry for five separate dikes. Three are nonmigmatitic, and two are migmatitic with 1-cm garnets and well-developed leucocratic segregations. The calculations use near-rim garnet compositions, just inward of reversals in Mg/(Mg+Fe), and averages of plagioclase and hornblende compositions, excluding reequilibrated rims (compositions for sample M61 are reported in Table 2). Because garnet and hornblende show some evidence for diffusional reequilibration, the calculated temperatures are probably minimum estimates. Peak temperatures were probably close to or above 800°C.

There is some uncertainty about the exact time at which these metamorphic conditions prevailed. From crosscutting relations and textural relationships described above, the dikes

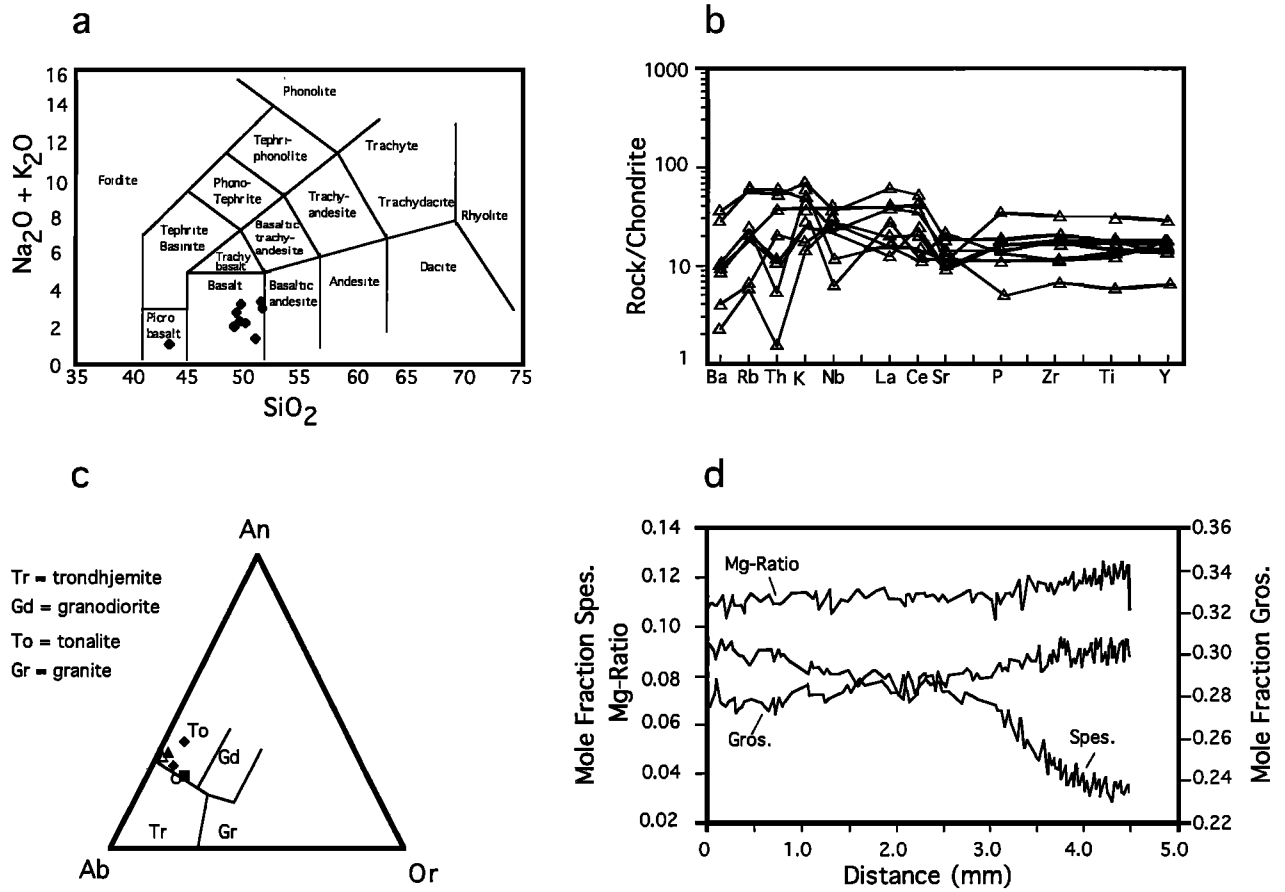

Figure 8. Major and trace element compositions of Chipman dikes and leucosomes. (a) Alkali-silica classification of *LeBas et al.* [1986] of nine separate dike samples; data from Table 1. (b) Spiderdiagram showing chondrite-normalized trace element profiles from the same nine dikes [after *Sun*, 1980 and *Wilson*, 1989]. (c) CIPW normative feldspar plot [after *Barker*, 1979], showing leucosome compositions. Open circle, average of 300 electron microprobe analyses of a single leucocratic tail (M61-P). All other analyses are by XRF: solid diamonds, leucocratic tails (M61,C26) associated with garnet; open triangle, small clean discrete segregation (C24-N); solid triangle, same segregation (C24-H) but with dispersed hornblende; solid square, mylonitic Chipman tonalite. (d) Microprobe traverse from core to rim of a 5-mm garnet from sample M61. See text for discussion.

underwent granulite facies metamorphism and migmatization at circa 3.2 Ga. However, the conditions (800°C, 1.0 GPa) are similar to those we have obtained for the northwestern domain and for the emplacement of the upper deck (M.L. Williams, unpublished data, 1992), both known to have occurred at circa 2.6 Ga. At present, we conclude that similar metamorphic conditions were reached on two occasions (3.2 and 2.6 Ga) in the southeastern domain. It is possible that the rocks were not substantially uplifted after the first event, and thus the two metamorphic events represent two thermal events superimposed on a generally counterclockwise P-T loop.

Some of the calculated P and T conditions are remarkably high considering the evidence for significant resetting of equilibria in other granulites [*Spear and Florence*, 1992; *Pattison and Bégin*, 1994]. The anomalous preservation of these conditions may be attributed to a number of factors. First, many of the garnet crystals used in the calculations are large, greater than 1 cm in diameter. Significant time would be required for diffusional reequilibration of these large crystals. Second, because these rocks contain abundant hornblende and pyroxene, the absolute magnitude of compositional change of these phases during reequilibration may not be large. Their present compositions may be near to their peak compositions, and thus in combination with the large garnet crystals, higher temperatures may be preserved. Further, peak metamorphic conditions apparently outlasted deformation. Late-stage (2.6 Ga) shearing was concentrated in narrow shear zones at the edge of the mylonite zone; little penetrative deformation occurred within the domain to assist retrograde reequilibration.

Discussion

Evidence for In Situ Anatexis

A number of lines of evidence indicate that the leucocratic segregations in the Chipman dikes representi in situ partial melts of the amphibolite dikes themselves. As with the migmatites described by *Sawyer* [1991], the similarity of major element compositions of migmatized and nonmigmatized dikes (Table 1) indicates that the leucosomes do not

Table 2. Microprobe Analyses of Major Phases in Migmatitic Dike for Sample M61

	Grt Core	Grt Rim	Hbl All	Bt All	Pl Matrix	Pl Melt
FeO	26.33	27.24	17.29	26.16	0.29	0.07
MgO	1.83	2.16	6.82	7.30	0.00	NA
MnO	4.12	1.40	0.33	0.23	0.00	NA
CaO	10.12	11.12	11.77	0.00	8.59	4.75
Na_2O	NA	NA	1.34	0.08	7.02	9.51
K_2O	NA	NA	1.39	8.99	0.10	0.12
TiO_2	NA	NA	1.52	2.43	0.00	NA
Fe_2O_3	NA	NA	5.40	0.00	0.00	NA
Al_2O_3	21.40	21.52	13.06	17.05	27.53	24.13
SiO_2	37.45	37.35	40.48	34.52	57.50	61.73
Total	101.25	100.79	99.40	96.76	101.03	100.31
			Cations			
Fe^{2+}	1.741	1.800	2.187	3.399	0.011	0.002
Mg	0.215	0.254	1.538	1.691	0.000	NA
Mn	0.276	0.094	0.043	0.030	0.000	NA
Ca	0.857	0.942	1.907	0.000	0.409	0.226
Na	NA	NA	0.394	0.024	0.605	0.817
K	NA	NA	0.268	1.781	0.005	0.007
Ti	NA	NA	0.173	0.284	0.000	NA
Fe^{3+}	NA	NA	0.614	NA	NA	NA
Al	1.994	2.005	2.328	3.122	1.442	1.260
Si	2.960	2.952	6.119	5.363	2.556	2.735
			End-Members, mol %			
Prp	7	8		Ab	59	78
Alm	56	58		An	40	22
Grs	28	30		Or	0	1
Sps	9	3				
Mg	0.11	0.12				

NA, not analyzed. Mg #, Mg/(Mg+Fe). Mineral abbreviations after *Kretz* [1983].

represent external felsic melts injected into the dikes. For example, sample M2432 contains at least 25% leucosome material. An addition of this amount of relatively pure quartz and plagioclase would be recognizable in comparison with a nonmigmatized dike such as M112. Instead, the data suggest that the leucosomes were derived internally.

The most compelling evidence for melting rather than a solid state origin comes from the complete progression that can be seen from incipient leucosomes with small garnets to larger leucosomes with larger garnets, to small pools and veins of leucosome, to large tonalite bodies (Figures 5 and 6). Additional textural evidence for melting includes the narrow leucosome trails which connect large garnet crystals without segregations to leucosome-filled boudin necks (Figures 6b and 6c) and variously misaligned fragments of dikes found in some leucocratic segregations (Figures 6d and 6e). Textures within the leucosomes generally reflect deformational processes, but the weak alignment of some large feldspars and the preservation of some straight crystal boundaries may be further evidence for melting. Finally, peak temperatures determined for the dike swarm (~800°C) are well with the range in which dehydration melting of amphibolite is predicted [*Percival*, 1983; *Sawyer*, 1991; *Wolf and Wyllie*, 1994].

Although very few analyses are available at present, trace element data from the leucosomes (Table 1) are not inconsistent with an origin by partial melting. As noted above, the data are similar to natural analyses and theoretical models presented by *Sawyer* [1991] for leucosomes interpreted to have resulted from anatexis. On the basis of these observations and the similarity of many characteristics of the Chipman migmatites to the results of recent experimental investigations of amphibolite anatexis (see below), we conclude that the Chipman dikes underwent vapor-absent melting to produce garnet and a tonalitic or trondhjemitic melt.

Comparison With Experimental Results

Recent field and experimental studies have clarified the phase relations of amphibolites during anatexis [*Percival*, 1983; *Ellis and Thompson*, 1986; *Rushmer*, 1991; *Rapp et al.*, 1991; *Beard and Lofgren*, 1991; *Sawyer*, 1991; *Wolf and Wyllie*, 1993; 1994]. The data suggest that at relatively low pressures, below 0.8 GPa, vapor-absent amphibolites can melt at temperatures of the order of 850-1000°C by reactions such as [*Rushmer*, 1991]

$$\text{Hbl} + \text{Pl} + \text{Qtz} = \text{Cpx} + \text{Ca-Pl} + \text{Melt} +/- \text{Ilm}. \quad (1)$$

At higher pressures (above approximately 0.8 GPa) garnet becomes an important product phase, with melting reactions

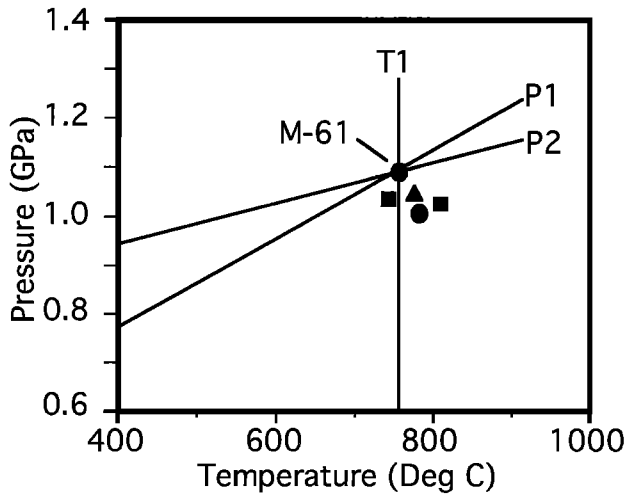

Figure 9. Thermobarometry of selected Chipman dikes. All estimates are based on garnet-hornblende-plagioclase quartz equilibria; equilibrium curves are plotted for only sample M61 (analyses from Table 2). Calculations assume that all iron is ferrous. T1: garnet-hornblende thermometer [*Graham and Powell*, 1984]; P1, P2, garnet-hornblende-plagioclase barometer, Mg and Fe end-member reactions [*Kohn and Spear*, 1989]. Solid circles, migmatitic dikes; solid squares, nonmigmatitic, cauliflower texture dikes; solid triangle, fine-grained undeformed dike with plagioclase phenocrysts and fine garnet (<1 mm). See Table 2 for compositions.

such as [*Percival*, 1983; *Rapp et al.*, 1991; *Wolf and Wyllie*, 1994]

$$\text{Hbl} + \text{Pl} = \text{Grt} + \text{Cpx} + \text{Melt}. \quad (2)$$

Theoretical and experimental data suggest that the higher-P, garnet-bearing, vapor-absent solidus may have a negative dP/dT slope such that partial melting of amphibolite at relatively high-P may occur at lower temperatures than melting at lower pressures [*Rushmer*, 1991; *Wolf and Wyllie*, 1994].

The Chipman dikes are clearly an example of relatively high-pressure partial melting. Calculated pressures are consistently near 1.0 GPa, and garnet is the dominant, and typically the only, new solid phase produced during anatexis. Experimental results of *Wolf and Wyllie* [1993; 1994] are particularly applicable to the Chipman dikes because these experiments were carried out at 1.0 GPa and starting compositions not unlike those of the Chipman dikes (Table 1), although Mg and Ca richer. On the basis of the experimental results, rough upper temperature limits can immediately be placed on anatexis in the Chipman dikes. Garnet is produced during partial melting only between approximately 800 and 1000°C; at lower and higher temperatures clinopyroxene is the dominant solid product phase.

It is interesting to note that the results of most recent studies, including those of *Wolf and Wyllie* [1993; 1994], indicate that a significant amount of clinopyroxene is produced along with garnet during high-P vapor-absent melting. In these experiments, there was a peak in the modal amount of garnet produced between 850 and 900°C, but this also corresponded to a peak in clinopyroxene production [*Wolf and Wyllie*, 1994, Figure 2]. Little or no clinopyroxene is present in the Chipman migmatites. To some degree this reflects the Fe-rich and Ca-poor composition of these amphibolites compared to those of Wolf and Wyllie. It is also possible that some clinopyroxene was produced during melting of the Chipman dikes and has now back-reacted to hornblende and plagioclase. Fine-grained clinopyroxene might be more readily retrograded than the large garnet crystals, many of which are partly replaced by hornblende and plagioclase. However, no clinopyroxene relics or inclusions have been found, and fine-grained clinopyroxene is stable and abundant in the nonmigmatitic, cauliflower texture dikes. We suspect that some clinopyroxene was produced during melting, but the bulk composition of the dikes greatly favored garnet.

Deformational Controls on Melt Segregation

Deformation played a key role in segregation of partial melts from the Chipman dikes. The segregation process apparently occurred in three stages: (1) small amounts of tonalite melt accumulated adjacent to garnet crystals, with the volume of melt proportional to the size of the garnet crystal; (2) small melt segregations became separated from their garnet crystals and coalesced into larger discrete pools in structurally favorable locations both in the dikes and in the adjacent tonalite; and (3) further shearing led to deformation of the melt pools, in the liquid and the solid state, interleaving new tonalite with the older already deformed tonalite, and presumably ejecting some melt upward into the overlying crust.

Stage 1: Partial melting and initial segregation. During the early stages of melting, partial melts collected in the low-strain shadows or sectors [*Hanmer and Passchier*, 1991], adjacent to garnet crystals in a variety of kinematic settings. In each setting, the low-strain sectors contain the instantaneous extension direction, i.e., the X direction of the flow. There are several ways in which these geometries might originate. *Wolf and Wyllie* [1993] suggested that garnets crystallize from the liquid within melt pods. If so, small melt segregations in the Chipman dikes may already have been flattened into the foliation when the garnet crystals nucleated. However, we favor a model in which garnet crystals nucleate away from the initial melt sites, and then the melt migrates into the low-strain sectors adjacent to the stiff garnets. It seems likely that small openings or gaps would develop adjacent to garnet in the instantaneous extension direction and be subsequently filled with melt [*Strömgård*, 1973]. Regardless of the mechanism, it is clear that the garnet-plus-tail geometry is established extremely early in the process because even the smallest, pinhead-sized garnets have recognizable melt tails.

Once the garnets were present, strain heterogeneity around the rigid garnet crystals apparently controlled the subsequent morphology of the melt domains. The liquid continued to collect in the instantaneous extension direction. It was probably forced toward these domains from the higher strain (higher mean stress?) domains in the matrix, particularly those adjacent to the garnets in the Z direction of instantaneous strain [see *Strömgård*, 1973; *Maaløe*, 1982; *Sawyer*, 1994]. It is interesting that few vestiges of the matrix minerals are present in most melt segregations. This indicates that extension occurs within, or at the edge of, the existing melt segregations, not within or between the matrix minerals. Thus the melt-filled pods continue to expand, filling with relatively uncontaminated partial melt.

The fact that the size of the melt segregations remains roughly proportional to the size of the garnet crystals indicates that at this early stage in the melting cycle, the source area for the melts is very local. That is, partial melts and their associated garnets were produced simultaneously from the same small domain of the dike. In migmatized dikes, there are no garnets without melt tails and no garnets with abnormally large tails. If two or more garnet crystals shared the same source volume, then it is unlikely that the size of the melt tails would be so closely linked to the size of the garnet crystals.

Stage 2: Migration and local segregation. At some point, the melts do become separated from their associated garnet crystals and collect into larger pools. This second stage of segregation is also dominantly structurally controlled and structurally driven. In many dikes, the process involves boudinage of dikes within the shearing tonalite matrix. It seems likely that the primary melt segregations associated with garnets affect the rheology of the dikes, leading to boudinage or fracturing and hence to the secondary melt segregations. However boudinage is neither a necessary result of melting nor a requirement for segregation. Although boudinage is more common in dikes with a significant amount of melting, it has been seen in dikes in all stages of the partial melting process, and melts were able to escape from some dikes that were not undergoing boudinage. The actual migration of melt from a host garnet crystal to a larger melt pool is probably driven by pressure gradients in the area surrounding the melt pool structures [see *Strömgård*, 1973; *Sawyer*, 1994]. Melts within a certain distance of a boudin neck or gash fracture are forced from the higher-pressure

garnet tails to the lower-pressure pools. This migration itself may lead to further dike failure and further mobilization.

Stage 3: Large-scale segregation and subsequent deformation. There is evidence that the same deformation that led to accumulation of the larger melt pools and segregations may have also served to expel the melts from the pools. Several examples of imbricated tabular dike segments have been recognized (see Figure 6d). Some of the segments are attenuated at their ends, suggesting that they originated as boudins during extension and then were subsequently thrusted and imbricated during a phase of layer-parallel shortening. Veins and streaks of felsic melt occur near the ends of the imbricated segments, suggesting that melt pools may have once been present in the boudin necks. If so, these melts were probably ejected during the subsequent shortening. Within the spatially and temporally heterogeneous patterns of flow, it is likely that dikes experienced periods of shortening and extension, and that melt pools were sporadically created and then forcibly emptied. Such a mechanism may serve to pump the newly formed felsic melts from their source rocks upward into the overlying crust.

Perhaps the most fundamental implication of the textures in the Chipman dikes is the critical role that deformation played in all stages of melt segregation. The melts appear to have been forcibly extracted from the dikes through a series of intermediate holding pools until they were mechanically mixed into the Chipman tonalite or were ejected from the system. Previous workers have focused on buoyancy, melt-induced fracturing, or rheological behavior of crystal+liquid systems in evaluating the amount of melt necessary for segregation and the mechanisms of melt transport [see *Miller et al.*, 1988; *Wickham*, 1987]. However, observations from the Chipman dikes and other regions [*Pattison and Harte*, 1988; *Sawyer*, 1994] suggest that buoyancy may only be of secondary importance during the early stages of melting and segregation. Instead, strain heterogeneities controlled by rheological variations in the host rocks and especially between the host rocks and melt segregations may be most important. Extremely small percentages of tonalitic melt (less than 1%) have been separated from their source regions and injected into structurally favorable sites [see *Maaløe*, 1982; *Dell'Angelo and Tullis*, 1988; *Sawyer*, 1991]. Buoyancy of the melt may become important after accumulation into larger pools. However, work on transport of magmas even in the lower and middle crust suggests that deformation may always be critically important [*Hollister and Crawford*, 1986; *Karlstrom et al.*, 1993; *Paterson and Fowler*, 1993].

Tectonic Speculations

The Chipman dike swarm was emplaced into the Chipman tonalite, during transpressive sinistral shearing, not long after the formation of the tonalite itself. Preliminary Sm-Nd data from the Chipman tonalite indicate that it may have developed in an arc-related environment [*Hanmer et al.*, 1995; C.F. Kopf, unpublished data, 1993]; and geochemical data from the dikes and the tonalite are broadly compatible with an arc or back arc setting. An ocean ridge setting, although compatible with the MORB-like composition and sheeted dike character of the terrane, is incompatible with the hydrous nature of the dikes, with the tonalitic host rocks, and with the transpressional deformational environment. We conclude that the dikes were emplaced into the base of a circa 3.2 Ga Archean island arc that developed between the Rae and the Hearne microcontinents during their amalgamation.

Granulite facies reaction textures are well-preserved in the Chipman dikes, but the origin of the parent hornblende-plagioclase assemblages is less clear. One possibility is that the dikes were emplaced as anhydrous gabbros or basalts, then hydrated to amphibolites, and finally metamorphosed and dehydrated during granulite facies metamorphism. However, field relations suggest that new dikes were sequentially emplaced while older dikes were undergoing deformation and dehydration metamorphism (i.e., Figure 8). This would require several cycles of dry dike emplacement, then hydration, then dehydration. Instead, we suggest that the igneous dikes were originally emplaced with a significant amount of water (i.e., in hornblende) into relatively dry granulite facies tonalite. Most of the dikes now contain approximately 30 to 40% hornblende which equates to somewhat less than 1% water, but more may have been present before the dikes crystallized and before dehydration and melting reactions occurred. Although some of the water could be primordial Archean mantle water, the interpreted arc setting for the dike/tonalite complex suggests that the water was probably introduced at an Archean subduction zone adjacent to the arc.

Not long after emplacement, some of the amphibolite dikes recrystallized to dry granulite (Grt-Cpx-Ilm) assemblages, but a large number of dikes underwent vapor-absent melting to produce garnet and a tonalitic or trondhjemitic melt. Temperatures in the Chipman tonalite at the time of dike emplacement were probably on the order of 800°C, but there may have been significant temperature variations associated with newly emplaced mafic and felsic melts. If new dikes were intruded at temperatures significantly above 800°C, they would be expected to have cooled and solidified against the 800°C tonalite. Because the dikes were hydrous, hornblende-bearing assemblages were stable under these conditions. This is suggested by the apparent stability of late stage fine-grained, undeformed amphibolite dikes with no evidence for melting. However, the emplacement of new dikes near newly solidified amphibolites would have elevated the temperature of the preexisting dikes. A temperature increase of only 50-100°C would be sufficient to cross the vapor-present or vapor-absent solidus, and initiate the melting reaction(s). The fact that some garnet crystals have undergone retrograde rehydration in the vicinity of leucocratic melt pools may be evidence that the ambient temperatures were not anomalously high. If background temperatures were below the vapor absent solidus, then small amounts of water released as the felsic melt crystallized could lead to the local reactions back to the stable amphibolite assemblage.

High geothermal gradients and high heat flows in arc complexes have been interpreted as resulting from mafic magmas that have been underplated and injected into the lower crust [*Oxburgh and Turcotte*, 1971; *Miyashiro*, 1973; *Harley*, 1989; *Ellis and Maboko*, 1992]. These underplated magmas may also be responsible for felsic plutonism and high-T, low-P metamorphism in the middle and upper parts of arc complexes [*Barton and Hanson*, 1989; *DeYoreo et al.*, 1989; *Sandiford and Powell*, 1991]. We interpret the Chipman dike swarm to have formed immediately above the Archean Moho and the underlying gravity anomaly to represent a mafic pluton that originated as a deep-crustal magma chamber or a body of underplated magma immediately below the crust. The dikes and the underlying magmas provided not only the amphibolite which underwent partial melting but also the heat required for the melting and for

granulite facies metamorphism. In this respect, the Chipman dike swarm may represent the often cited but seldom seen source for metamorphic heat in the magmatic arc setting. It may be the top part of the region of advective heat and mass transfer from mantle to crust.

The Chipman tonalite and Chipman dike swarm offer a somewhat different scenario for the development of tonalite than other Archean tonalite-trondhjemite-granodiorite (TTG) terranes. Other workers have suggested that the early crust was mafic and locally amphibolitic and that TTG plutons developed through partial melting of this early crust [see *Rapp et al.*, 1991, and references therein]. Although this model may explain the generation of the parental Chipman tonalite, a significant amount of tonalite magma was produced from dikes injected into this tonalite. In this region, the oldest rocks are tonalites, and much of the mafic component in the tonalite does not represent vestiges of an original parental mafic crust but instead represents vestiges of partially melted and digested mafic dikes. The early evolution of Archean tonalite may not have been a single progression from mafic to TTG rocks. Instead, it may have involved multiple cycles of tonalite production, injection of new mafic rocks, and partial melting and rehomogenization of the composite tonalite.

Acknowledgments. The authors wish to thank M. Nyman, D. Pattison, and E. Sawyer for careful and insightful reviews of this manuscript. David Snoeyenbos and Sheila Seaman are thanked for helpful discussions at all stages of the research and for careful reviews of several earlier drafts. The work was supported by NSF grant EAR-9106001 to Williams. Fieldwork during 1990 and 1991 was supported by the Geological Survey of Canada. This paper is Geological Survey of Canada contribution 68594.

References

Ashworth, J.R., and M. Brown (Eds.), *High-Temperature Metamorphism and Crustal Anatexis*, 407 pp., Unwin Hyman, Boston, Mass., 1990.

Barker, F., Trondhjemites: Definition, environment, and hypotheses of origin, in *Trondhjemites, Dacites, and Related Rocks*, edited by F. Barker, pp. 1-12, Elsevier, New York, 1979.

Barton, M.D., and R.B. Hanson, Magmatism and the development of low-pressure metmorphic belts: Implications from the western United States and thermal modeling, *Geol. Soc. Am. Bull., 101*, 1051-1065, 1989.

Beard, J.S., and G.E. Lofgren, Dehydration melting and water-saturated melting of basaltic and andesitic greenstones and amphibolites at 1, 3, and 6.9kb, *J. Petrol., 32*, 365-401, 1991.

Berthe, D., P. Choukroune, and P. Jegouzo, Orthogneiss, mylonite and noncoaxial deformation of granites: the example of the South Armorican Shear Zone, *J. Struct. Geol., 1*, 31-42, 1979.

Brown, M., The generation, segregation, ascent and emplacement of granitic magma: The migmatite to crustally-derived granite connection in thickened orogens, *Earth Sci. Rev., 36*, 8-130, 1994.

Dell'Angelo, L.N., and J. Tullis, Experimental deformation of partially melted granitic aggregates, *J. Metamorph. Geol., 6*, 495-516, 1988.

DeYoreo, J.J., D.R. Lux, and C.V. Guidotti, The role of crustal anatexis and magma migration in regions of thickened continental crust, in *Evolution of Metamorphic Belts*, edited by J.G. Daly, R.A. Cliff, and B.W.D. Yardley, pp. 187-202, Blackwell Scientific, Cambridge, Mass., 1989.

Ellis, D.J., and M.A.H. Maboko, Precambrian tectonics and the physiochemical evolution of the continentl crust, I, The gabbro eclogite transition revisited, *Precambrian Res., 55*, 491-506, 1992.

Ellis, D.J., and A.B. Thompson, Subsolidus and partial melting reactions in the quartz-excess $CaO+MgO+Al_2O_3+SiO_2+H_2O$ system under water-excess and water deficient conditions to 10 kb: Some implications for the origin of peraluminous melts from mafic rocks, *J. Petrol.*, 27, 91-121, 1986.

Fyfe, W.S., The granulite facies, partial melting and the Archean crust, *Philos. Trans. R. Soc. London A*, 273, 457-461, 1973.

Gamond, J.F., Displacement features associated with fault zones: A comparison between observed examples and experimental models, *J. Struct. Geol., 5*, 33-46, 1983.

Giret, A., B. Bonin, and J.M. Leger, Amphibole compositional trends in oversaturated and undersaturated alkaline plutonic ring-complexes, *Can. Mineral., 18*, 481-495, 1980.

Goodacre, A.K., R.A.F. Grieve, J.F. Halpenny, and V.L. Sharpton, Horizontal gradient of the Bouguer gravity anomaly map of Canada, *Canadian Geophysical Atlas, Map 5, scale 1:10,000,000, Geol. Surv. Can.*, Ottawa, 1987.

Graham, D.M., and R. Powell, A garnet-hornblende geothermometer: Calibration, testing, and application to the Pelona Schist, southern California, *J. Metamorph. Geol., 2*, 13-21, 1984.

Hanmer, S., Ductile thrusting at mid-crustal level, southwestern Grenville Province, *Can. J. Earth Sci., 25*, 1049-1059, 1988.

Hanmer, S., Geology, East Athabasca mylonite triangle, Stony Rapids area, northern Saskatchewan, parts of NTS 740-O and 74-P, *Geol. Surv. Can. Map 1859A, scale 1:100,000, Geol. Surv. Can.*, Ottawa, 1994.

Hanmer, S., Geology of the Striding-Athabasca mylonite zone, northern Saskatchewan and southeast District of Mackenzie, *Geol. Surv. Can. Mem.*, in press, 1995.

Hanmer, S., and C. Kopf, The Snowbird tectonic zone in District of Mackenzie, Northwest Territories, in *Current Research, Part C, Pap. Geol. Surv. Can.*, 93-1C, 41-52, 1993.

Hanmer, S., and C.W. Passchier, Shear-sense indicators a review, *Pap. Geol. Surv. Can., 90-17*, 1991.

Hanmer, S., M. Darrach, and C. Kopf, The East Athabasca mylonite zone: an Archean segment of the Snowbird tectonic zone in Northern Saskatchewan, in *Current Research, Part C, Pap. Geol. Surv. Can., 92-1C*, 19-29, 1992.

Hanmer, S., C. Kopf, R. Parrish, and M. Williams, Striding-Athabasca mylonite zone, I, Complex Archean deep crustal deformation in the East Athabasca Mylonite Triangle, N. Saskatchewan, *Can. J. Earth Sci. 31*, 1287-1300, 1994.

Hanmer, S., Williams, M., and Kopf, C., Striding Athabasca mylonite zone: Implications for the Archean and Early Proterozoic tectonics of the western Canadian Shield, *Can. J. Earth Sci., 32*, 178-196, 1995.

Harley, S.L., The origins of granulites: A metamorphic perspective, *Geol. Mag., 126*, 215-331, 1989.

Hoffman, P.F., United Plates of America, the birth of a craton: Early Proterozoic assembly and growth of Laurentia, *Ann. Rev. Earth Planet. Sci., 16*, 543-603, 1988.

Hollister, L.S., and M.L. Crawford, Melt-enhanced deformation: A major tectonic process, *Geology, 14*, 558-561, 1986.

Karlstrom, K.E., C.F. Miller, J.A. Kingsbury, and J.L. Wooden, Pluton emplacement along an active ductile thrust zone, Piute Mountains, southeastern California: Interaction between deformational and solidification processes, *Geol. Soc. Am. Bull., 105*, 213-230, 1993.

Kohn, M.J., and F.S. Spear, Empirical calibration of geobarometers for the assemblage garnet + hornblende + plagioclase + quartz, *Am. Mineral., 74*, 77-84, 1989.

Kretz, R., Symbols for rock-forming minerals, *Am. Min., 68*, 277-279, 1983.

Leake, B.E., Nomenclature of amphiboles, *Can. Mineral., 16*, 501-520, 1978.

LeBas, M.J., R.W. LeMaitre, A. Streckeisen, and B. Zanettin, A

chemical classification of volcanic rocks based on the total alkali-silica diagram, *J. Petrol., 27*, 745-750, 1986.

Logan, J.M., Brittle phenomena, *Rev. Geophys., 17*, 1121-1132, 1979.

Maaløe, S., Geochemical aspects of permeability controlled partial melting and fractional crystallization, *Geochim. Cosmochim. Acta, 46*, 43-57, 1982.

Macdonald, R., New edition of the geological map of Saskatchewan, Precambrian Shield area, in *Summary of Investigations,* pp. 19-21, in *Sask. Geol. Surv.*, Regina, 1980.

Miller, C.F., E.B. Watson, and T.M. Harrison, Perspectives on the source, segregation and transport of granitoids, *Trans. R. Soc. Edinburgh Earth Sci., 79*, 135-156, 1988.

Miyashiro, A., *Metamorphism and Metamorphic Belts*, 492 pp., John Wiley, New York, 1973.

Myers, J.S., Formation of banded gneisses by deformation of igneous rocks, *Precambrian Res., 6*, 43-64, 1978.

Oxburgh, E.R., and D.L. Turcotte, Origin of paired metamorphic belts and crustal dilation in island arc regions, *J. Geophys. Res., 76*, 1315-1327, 1971.

Passchier, C.W., and C. Simpson, Porphyroclast systems as kinematic indicators, *J. Struct. Geol., 8*, 831-844, 1986.

Paterson, S.R., and T.K. Fowler, Re-examining pluton emplacement processes, *J. Struct. Geol., 15*, 191-206, 1993.

Pattison, D.R.M., and N.J. Bégin, Zoning patterns in orthopyroxene and garnet in granulites: Implications for geothermometry, *J. Metamorph. Geol., 12*, 387-410, 1994.

Pattison, D.R.M., and B. Harte, Evolution of structurally contrasting anatectic migmatites in the 3-kbar Ballachulish aureole, Scotland, *J. Metamorph. Geol., 6*, 475-494, 1988.

Percival, J.A., High-grade metamorphism in the ChapleauFoleyet area, Ontario, *Am. Mineral., 68*, 667-686, 1983.

Rapp, R.P., E.B. Watson, and C.F. Miller, Partial melting of amphibolite/eclogite and the origin of Archean trondhjemites and tonalites, *Precambrian Res., 51*, 1-25, 1991.

Robinson, P., F.S. Spear, J.C. Schumacher, J. Laird, C. Klein, B.W. Evans, and B.L. Doolan, Phase relations of metamorphic amphiboles: Natural occurrence and theory, in *Amphiboles: Petrology and Experimental Phase Relations, Rev. Mineral. Ser. 9B,* edited by D.R. Veblen, and P.H. Ribbe, pp. 1-227, Mineralogical Society of America, Washington, D.C., 1982.

Rushmer, T., Partial melting of two amphibolites: Contrasting experimental results under fluid-absent conditions, *Contrib. Mineral. Petrol., 107*, 41-59, 1991.

Sandiford, M., and R. Powell, Some remarks on hightemperature, low-pressure metamorphism in convergent orogens, *J. Metamorph. Geol., 9*, 333-340, 1991.

Sawyer, E.W., Disequilibrium melting and the rate of melt-residuum separation during migmatization of mafic rocks from the Grenville Front, Quebec, *J. Petrol., 32*, 701-738, 1991.

Sawyer, E.W., Melt segregation in the continental crust, *Geology, 22*, 1019-1022, 1994.

Sibson, R.H., Transient discontinuities in ductile shear zones, *J. Struct. Geol., 2*, 165-171, 1980.

Snoeyenbos, D.R., and M.L. Williams, An Archean eclogite facies terrane from the Snowbird tectonic zone, northern Saskatchewan, *Eos, 75 (16),* Spring Meeting suppl., 355, 1994.

Spear, F.S., and F.P. Florence, Thermobarometry in granulites: Pitfalls and new approaches, *Precambrian Res., 55*, 209-241, 1992.

Strömgård, K., Stress distribution during formation of boudinage and pressure shadows, *Tectonophysics*, 16, 215-248, 1973.

Sun, S., Lead isotopic study of young volcanic rocks from mid-ocean ridges, ocean islands, and island arcs, *Philos. Trans. R. Soc. London A, 297*, 409-445, 1980.

Whitney, J.A., The origin of granite: The role and source of water in the evolution of granitic magmas, *Geol. Soc. Am. Bull., 100*, 1886-1897, 1988.

Wickham, S.M., The segregation and emplacement of granitic magmas, *J. Geol. Soc. London, 144*, 281-297, 1987.

Wilson, M., *Igneous Petrogenesis*, 466 pp., Unwin Hyman, Boston, Mass., 1989.

Winther, K.T., and R.C. Newton, Experimental melting of hydrous low-K tholeiite: Evidence on the origin of Archean cratons, *Bull. Geol. Soc. of Den., 39*, 213-228, 1991.

Wolf, M.B., and J.B. Saleeby, Jurassic Cordilleran dike swarm-shear zones: Implications for the Nevadan orogeny and North American plate motion, *Geology, 20*, 745-748, 1992.

Wolf, M.B., and P.J. Wyllie, Garnet growth during amphibolite anatexis: Implications of a garnetifeous restite, *J. Geol., 101*, 357-373, 1993.

Wolf, M.B., and P.J. Wyllie, Dehydration-melting of amphibolite at 10kbar: The effects of temperature and time, *Contrib. Mineral. Petrol., 115*, 369-383, 1994.

Wyllie, P.J., Experimental studies on biotite- and muscovite-granites and some crustal magmatic sources, in *Migmatites, Melting and Metamorphism*, edited by M.P. Atherton, and C.D. Gribble, pp. 37-51, Shiva, Cambridge, Mass., 1983.

M. Darrach, C. Kopf, and M.L. Williams, Department of Geology and Geography, University of Massachusetts, Morrill Science Center, Box 35820, Amherst, MA 01003-5820. (e-mail: mlw@probe.geo.umass.edu)

S. Hanmer, Continental Geoscience Division, Geological Survey of Canada, 601 Booth St., Ottawa, Ont., Canada K1A 0E8.

(Received August 18, 1994; revised February 22, 1995; accepted February 28, 1995.)